Distribution of Content in Recently-Viewed Scenes Whitens Perception

April M. Schweinhart[1*], Patrick Shafto[1], and Edward, A. Essock[2]

[1]Department of Mathematics and Computer Science
Smith Hall, Room 216, 101 Warren St
Rutgers, The State University of New Jersey
Newark, NJ 07102

[2]Department of Psychological and Brain Sciences
317 Life Science Building
University of Louisville
Louisville, KY 40292

*Correspondence to:
Smith Hall, Room 216, 101 Warren St
Rutgers, The State University of New Jersey
Newark, NJ 07102
(502) 439-0557
schweinharta@gmail.com

Abstract

Anisotropies in visual perception have often been presumed to reflect an evolutionary adaptation to an environment with a particular anisotropy. Here we adapt observers to globally-atypical environments presented in virtual reality to assess the malleability of this well-known perceptual anisotropy. Results showed that the typical bias in orientation perception was in fact altered as a result of recent experience. Application of Bayesian modeling indicates that these global changes of the recently-viewed environment implicate a Bayesian prior matched to the recently experienced environment. These results suggest that biases in orientation perception are fluid and predictable, and that humans adapt to orientation biases in their visual environment "on the fly" to optimize perceptual encoding of content in the recently-viewed visual world.

Keywords: Horizontal Effect, Visual Perception, Bayesian Modeling, Virtual Reality

Introduction

Humans are confronted by a visual world whose structure is biased in a number of ways. It has been argued previously that the neural encoding of complex scenic properties may be made efficient or "sparse" by taking such biases into account (Attick & Redlich, 1990; Barlow, 1989; Bex, Soloman, & Dakin, 2009; Brenner, Bialek, & de Ruyter van Steveninck, 2000; Field & Brady, 1997; Hansen & Essock, 2004; Wainwright, 1999). It has been further argued that visual experience with these biases, such as the distribution of spatial scales and colors of content in recently-viewed visual scenes, adapts our visual system to discount them and keep perceptions veridical in the face of changing environments (Cecchi, Rao, Xiao, & Kaplan, 2010; Shepard, 1992; Webster & MacLeod, 2011; Webster & Miyahara 1997). Take for example, the natural yellowing of an individual's lens across decades of age: the individual's perceptual encoding mechanisms also change to maintain an unchanging perception of "neutral" (Webster, Werner, & Field, 2005). Another fundamental property of the visual world, orientation of structural content in the scene, also has a biased distribution: typical scenes, both natural and "carpentered", are biased with more/stronger content at some orientations than others (Baddeley & Hancock, 1991; Coppola, Purves, McCoy, & Purves, 1998; Girshick, Landy, & Simoncelli, 2011; Hancock, Baddeley, & Smith, 1992; Keil & Cristobal, 2000; Switkes, Mayer, & Sloan, 1978; see review in Hansen and Essock, 2004). Specifically, due to the horizon, foreshortening, and phototropic/gravitropic growth (even aside from additional, "carpentered world" properties), the average scene contains most content around horizontal, second most around vertical and least near the oblique orientations (45° and 135°: Hansen & Essock, 2004). The processing of orientation in the human visual system is biased in the opposite way: suppression by content in a broadband image is strongest for horizontal content, least for oblique content, and intermediate for vertical content (Essock, DeFord, Hansen, & Sinai, 2003; Essock, Haun, & Kim, 2009; Hansen & Essock, 2004; Hansen & Essock, 2006). This *horizontal effect* pattern of anisotropy [1]

[1] The term *horizontal effect* refers to the general pattern of H>V>Ob found in measures of: magnitude of suppression by broadband patterns on an oriented target; perceptual threshold (inverse sensitivity) to oriented content in natural scenes and other broadband content; and amount/magnitude of oriented content contained in averaged natural scenes. The term follows the nomenclature of the term *oblique effect*, the anisotropy of performance observed on many tasks in which performance is *worst* for oblique stimuli and best for horizontal and vertical stimuli (Appelle, 1972). Thus, an oblique effect is shown in the sensitivity to isolated stimuli (e.g., grating, Gabor) but when broadband content is present a horizontal effect is observed due

is seen in suppression (both surround and overlay suppression, as well as general, large-field, suppression) and roughly matches the magnitude of the anisotropic bias (H>V>Ob) observed in average scene content (Essock, Haun, & Kim, 2009). This anisotropic suppression would be an efficient way for humans to encode orientation, whitening the neural representation, and serving to perceptually emphasize scene content (objects) that deviates structurally from the normal background of scenes (e.g., Essock et al., 2003; Hansen & Essock 2004; 2005; Essock et al., 2009; Hansen et al., 2015). However, it is not yet known if this horizontal-effect pattern of anisotropic suppression serves to undo the orientation-biased content on a long-term (e.g., evolutionary) timescale or a recent-past timescale, perhaps even adjusting perception of oriented structure 'on the fly' based on the current visual world. Here, we addressed whether the human visual system alters the perceptual salience of oriented structure to compensate for the distributions of oriented content in the just-experienced visual world. We evaluated this idea in the context of a previously developed Bayesian model of malleable orientation salience in which perceptual bias and variability are related to the prior expectations and likelihood of a given orientation of content in the environment (Girshick, Landy, & Simoncelli, 2011; Stocker & Simoncelli, 2006). Under this approach, the parameterization of the likelihood is inferred from observers' behavior and the prior probability is modeled from the empirically observed distribution of orientation content in the environment.

If it is the anisotropy in the *recently-viewed* environment that determines observers' internal prior probability distributions and in turn causes the perceptual anisotropy, then changing the environmental distribution should lead to changes in observers' perception of oriented structure which could be modeled via changes in the observer's prior probability of different orientations. We were specifically interested in testing how observers' perception would change after experience in an environment that was not biased across orientation (as are typical scenes), but instead was isotropic. As a follow-up, we also tested a subsample of three observers in two other globally-altered environments.

---

to the anisotropic masking (Hansen & Essock, 2006). Note also, that here we are referring to the "Class 1" oblique effect that reflects basic visual ability, *per se*, rather than the "Class 2" oblique effect that occurs on tasks that involve memory/recall of orientation of stimuli presented via any of several sensory modalities (Balikou, et al., 2015; Baud-Bovy, Gentaz, 2012; Essock, 1980; Essock, Krebs & Prather, 1997; Maloney & Clifford, 2015; Smyrnis, Mantas & Evdokimidis, 2014)

Methods

Observers

A total of nine subjects participated in the main experiment as preliminary power tests indicated at least 6 observers were necessary and no stopping rule was implemented. The nine observers (mean age of 23.6 years; 4 female; 7 naïve) were students at the University of Louisville. Experiments were conducted and consent obtained as per a protocol approved by the University's IRB. All observers were pre-screened to ensure normal or corrected-to-normal vision. One subject was dropped from the study after reporting nausea when wearing the head-mounted display.

Procedure

To determine the effect that adapting to different distributions of environmental statistics has on perception of orientation, nine observers' perceptual ability was measured at cardinal and oblique orientations (0º, 45º, 90º, 135º, clockwise from vertical) using a broadband, suprathreshold matching paradigm (Figure 1A) before and after adaptation in an isotropic environment presented in virtual reality (Figure 2). Observers were asked to adjust the increment of an oriented test pattern to "match the perceived 'strength' or 'salience' of the oriented structure" that they observed in a reference pattern which had a different (22.5^{o}) orientation (Figure 1A). This matching task is known to reveal a robust horizontal effect in that people perceive oblique contours as strongest and horizontal content as least salient in such broadband patterns (Hansen & Essock, 2004). Perceptual salience was measured again immediately after the adaptation period using the same task.

Test Stimuli

Two circular patches of oriented visual noise were simultaneously presented to the observer. One served as a test stimulus, the other as a reference. The 6.25^{o} patches were presented at eye level, centered 16.9^{o} apart and viewed through apertures in a large circular mask that occluded monitor bezels and other room structure (Figure 1A, right). The stimuli were viewed in an otherwise dark room. Observers were positioned by a chin/forehead rest at 2.37 M. The stimulus patches (512 pixels in diameter) consisted of broadband $1/f$ noise patterns with an incremented band of orientations (Figure 1A and B). These patterns were constructed in Matlab 8.2 in the

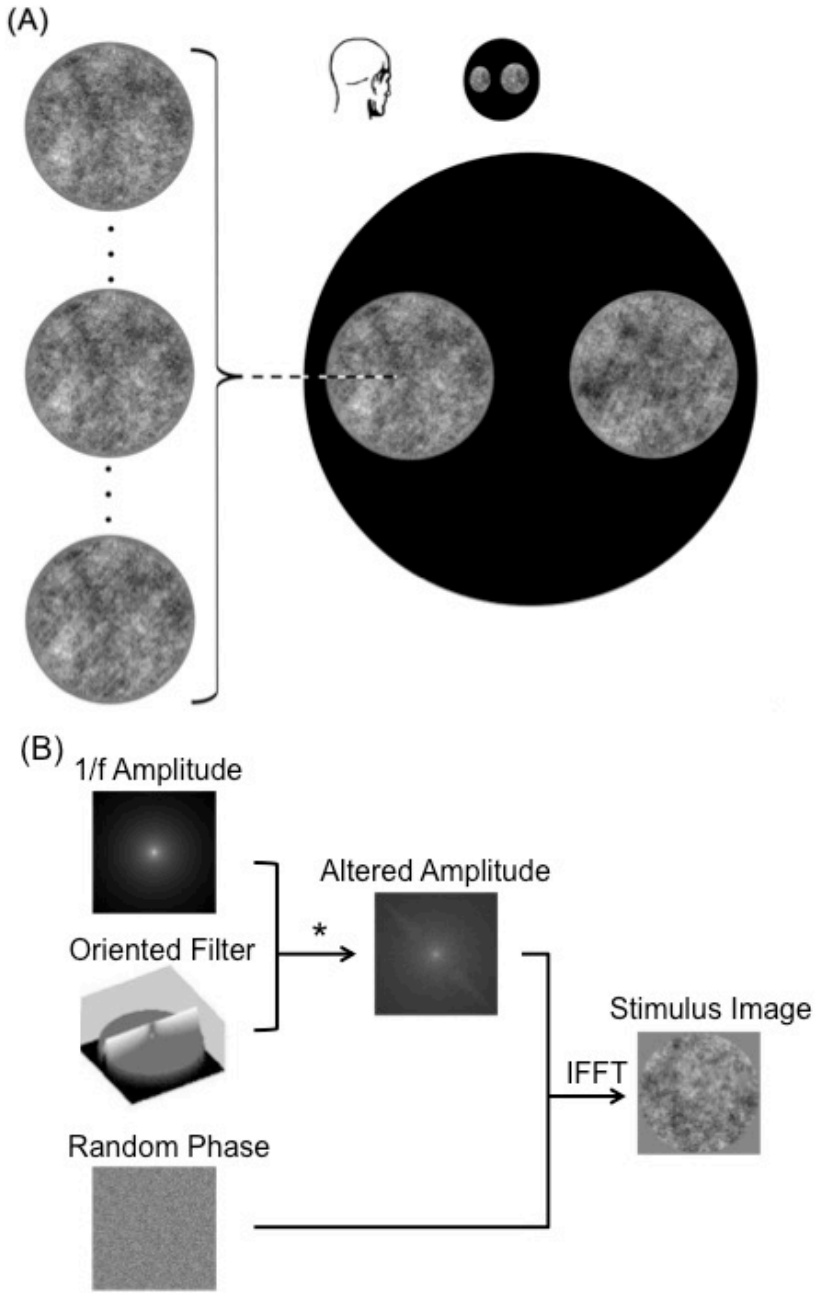

Figure 1. (A) Stimulus presentation. Left: Three examples of a 45° increment with different magnitudes of the oriented increment (I_{SC}) are shown; increments increase from the top to the bottom (I_{SC} = 1.3, 1.6, and 1.9). Right: Observer's view of stimuli to be matched. On a given trial the subject saw a test patch (left patch, shown at the 45° test orientation) whose increment they varied to match the magnitude of the oriented content in the standard stimulus (right patch, fixed to I_{SC} =1.6 and 22.5°). (B) Creation of spatially-broadband, oriented noise stimuli as seen in (A). An isotropic 1/f amplitude spectrum and a phase spectrum of random phase values were created. The isotropic amplitude spectrum was given an oriented component by multiplying it by an oriented filter thereby incrementing amplitude within a 20°-wide band of orientations, Following an inverse FFT, stimuli were cropped to a circle to form the stimulus patch. See text.

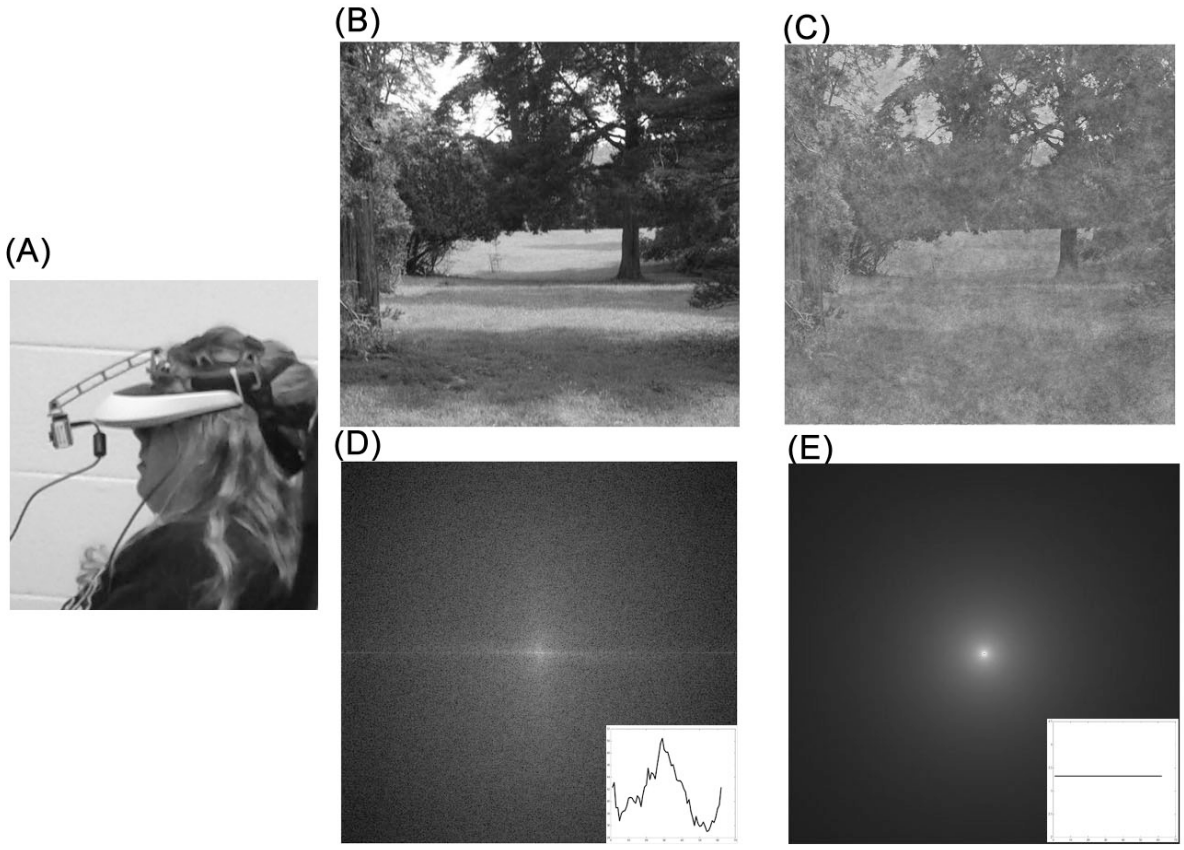

Figure 2. Image acquisition and processing. (A) During adaptation, the image of the visual environment was acquired through the camera and sent for processing to a laptop stored in a backpack that the observer wore. The image filtering process consisted of taking the original image (B) and performing a fast Fourier transform (FFT). The resulting amplitude spectrum (D) was replaced with an isotropic spectrum (E) and the frequency representation was inversed (IFFT) to create the new image (C) that was then sent to the HMD for viewing in near real-time.

Fourier domain by multiplying an amplitude matrix whose values fell off exponentially with spatial frequency (a "1/f pattern") by an oriented filter. The filter was triangular in orientation, peaking at the test orientation and falling off linearly to 1.0 on either side of the 20º-wide orientation band (see Figure 1B). (A triangle filter was used to avoid an orientation illusion, frequency-domain Mach Bands, generated by an abrupt edge in the orientation dimension (Essock, Hansen, & Haun, 2007)). For the "standard" (i.e., reference) stimulus, the peak of the orientation filter was an increment of 60% (an increment scalar, I_{SC}, of 1.6; see Figure 1B) and unchanged throughout the experiments. For the "test" stimulus, the starting increment at the beginning of each trial was randomly determined to be between 1.3 and 1.9 times the amplitude

of the background (and subsequently adjusted by the observers). Following the multiplication of the 1/f amplitude spectrum and the orientation filter, the resulting amplitude spectrum was combined with a 512 x 512 matrix of random phase values ranging from $-\pi$ to π and then inverse Fourier transformed to create the stimulus images (Figure 1B). Standard stimuli were presented on a Nanao Flexscann F2-21 20" CRT monitor and test stimuli were presented on a Samsung Syncmaster 1100 20" CRT monitor. Monitors were calibrated to express linear luminance values and were well matched (r^2= .998). Standard stimuli (Figure 1A) were presented with an orientation increment at 22.5º (stimuli were vertical on a monitor that was fixed at a 22.5º physical position).

On each trial the phase spectrum of the background noise was determined randomly and used for both the test and standard. Observers adjusted the increment of the test stimulus by increasing or decreasing the amplitude increment by computer keypress with both large (.1) and small (.05) steps available. Test orientation on each trial was block-randomized within blocks of four trials. The ratio of the increment needed for the observer to perceptually match the test orientation to the 22.5º standard's fixed increment was obtained over repeated trials and averaged. Pre-adaptation testing consisted of 36 trials (9 per test orientation) with the four test orientations block randomized. In the post-adaptation testing, observers completed as many trials of the matching task as possible in a 30-minute testing session. The mean and standard deviation of the observers' match values were taken to reflect the internal perceptual bias and perceptual variability, the latter of which was used to derive the parameters of the likelihood (Girshick, Landy, & Simoncelli, 2011).

Adaptation Paradigms and Analyses

During adaptation, the observer's view of his or her immediate environment was captured by a head-mounted digital camera, digitally altered, and then displayed in a head-mounted display (HMD) for real-time viewing (see Figure 2 and also Bao, Fast, Mesik, & Engel, 2013; Zhang, et al, 2009). Making the natural amplitude spectrum isotropic maintained the basic structure of the image (as structural relations are determined largely by the phase spectra, Morgan, Ross, & Hayes, 1991; Shapley, et al.,1990) but provided a natural-looking scene that was ensured to have an equal amount of structure (amplitude) at all orientations at each particular spatial frequency (see example in Figure 2). During the adaptation periods observers were allowed to move freely

and pursue any desired activity. Most sat and watched videos for much of the adaptation phase, although all observers were encouraged to move around and engage with the environment.

Observers wore a HMD (Sony HMZ-T2 Personal 3D Viewer) with a lightweight, black and white digital camera (NET CMOS iCube USB 3.0; 54.9° X 37.0° FOV) attached. The current visual environment that an observer was experiencing was acquired through the camera and sent to a laptop computer (HP ENVY 15t-j100) which filtered the camera images frame by frame and streamed the filtered images to the HMD to be viewed in near real-time (35 msec delay) by the observer as he/she interacted with the environment (Bao et al., 2013; Zhang et al., 2009). The viewer had a standard display gamma and a maximum luminance of 200 cd/m^2. All image filtering took place in Matlab (MATLAB 8.2, The MathWorks Inc., Natick, MA, 2013) using the *image acquisition*, *signal processing*, and *image processing* toolboxes applied to the pixel values. Each frame of the video output was fast Fourier transformed (FFT) and the resulting amplitude spectrum was replaced with a naturalistic (1/*f*), but isotropic spectrum (see Figure 2). The isotropic spectrum was then combined with the original phase spectrum of each frame and inverse transformed to be presented on the HMD. Two follow-up conditions, an "oblique-dominant" and an "enhanced-natural" condition, were also tested.[2] In the oblique-dominant condition a triangular filter (positive and negative) that attenuated cardinal and enhanced oblique amplitudes (equally at all spatial frequencies) within 45°-wide bands of orientations was multiplied with each frame's amplitude spectrum (see Figure 3B). The 45°-wide triangles had a peak amplitude of a factor (I_{SC}) of 1.95 at 45° and 135° and a minimum amplitude of a factor of 0.15 at 0° and 90°. For the enhanced natural condition the filter had

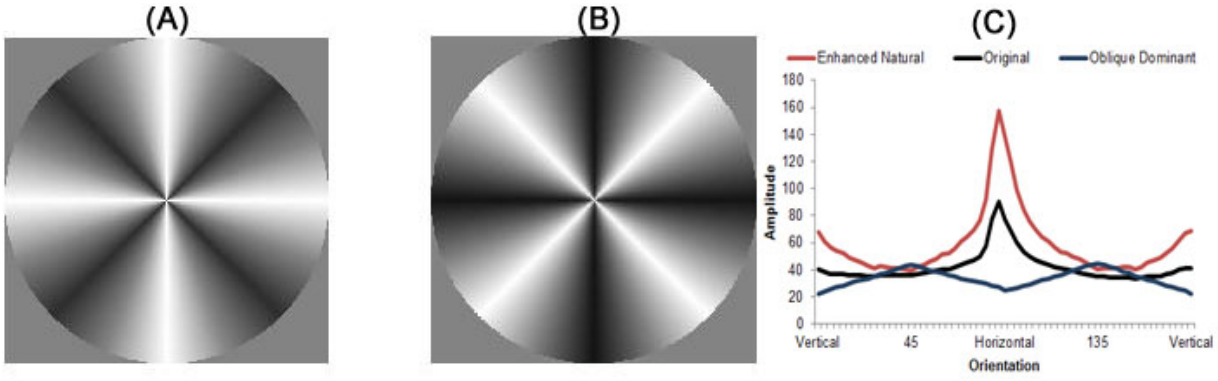

[2] A check verified that a given global filter had substantially the same effects on orientation when considered on a more-local (6.25°) scale.

Figure 3. The filters used during the "enhanced-natural" (A) and "oblique-dominant" (B) adaptation conditions, and (C) the resulting amplitude spectra when the filters are applied to a particular scene (the average of the adaptation period scenes is used here; see text).

peaks of 1.95 at 0^o and 90^o and minima of 0.35 at 45^o and 135^o (Figure 3A). Observers did not wear the device in either pre- or post-adaptation perceptual testing. A control condition of wearing the HMD for the 2-hour period with the visual input sham-filtered verified that there was no effect of the filtering/viewing process itself on orientation salience.

A digital recording of the environmental imagery that each subject was exposed to during adaptation was archived and used to characterize typical visual experience for modeling purposes. As the video recording lasted the entire adaptation period, the recordings were prohibitively large for full analysis, so a sample consisting of every 1/1000 frame was taken, FFT performed, and averaged. The average orientation spectrum from each sample of filtered and unfiltered images was computed by the method reported previously (Schweinhart & Essock, 2013; see *Modeling: Prior* for further details). The unfiltered orientation spectrum from these frames served as a 'typical' environmental distribution, that is, the mean of what the observer would have been exposed to without the filtering process being performed (Figure 3C).

Results

Perceptual Performance

All observers showed a horizontal effect in the pre-test: subjects needed a smaller physical increment (I_{SC}) in oblique stimuli, and a larger physical increment in horizontal stimuli to match the reference pattern before adaptation. After experience in an environment with isotropic orientation content, observers showed reliable and predictable changes in orientation perception. As adaptation effects diminished after 5-10 minutes, we calculated the observer's mean match over the initial five minutes after adaptation and used these values for all analyses. Following adaptation observers showed a significantly different pattern of perceived salience of oriented structure than they did before adaptation (Figure 4A, $F(3,48) = 11.05$, $p < .001$, $\eta^2 = 0.4$). To characterize the horizontal effect we calculated its magnitude as the horizontal match value divided by average oblique match value. After experiencing the isotropic environment every subject showed a reduced horizontal-effect pattern such that the magnitude of the biased perception reduced to an average near zero (Figure 4B, $t(8) = 3.23$, $p = .006$, $d = 1.06$). That is,

the well-known unequal perceptual salience of structure at different orientations disappeared after viewing an isotropic environment for two hours.

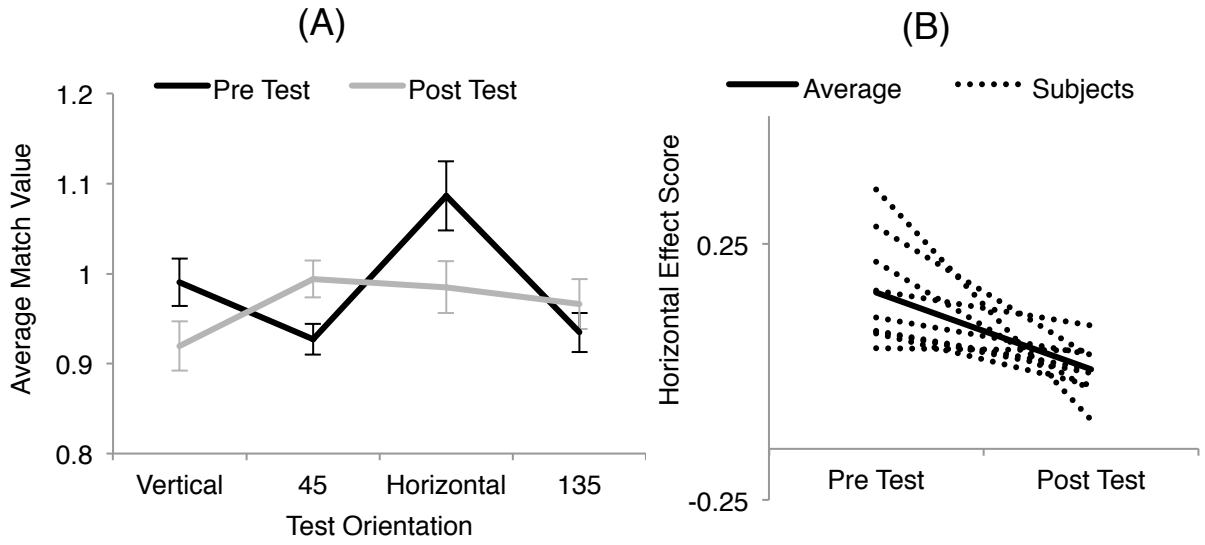

Figure 4. Measures of perceptual salience of oriented content before and after adaptation (N=9). (A) Average of the observers' perceptual salience across orientation before and after experience in an isotropic environment. Error bars represent ±1 standard error. (B) Horizontal effect score for each observer and group average (solid line) decreases after experience in an isotropic environment.

This malleable perception in response to changing environmental bias was also shown across other types of environmental change: in addition to adaptation to an isotropic visual environment we also adapted three of the observers to two other altered environments. Adaptation to an environment in which the typical anisotropy was increased (enhanced natural) caused orientation perception to become more anisotropic for each observer and adapting to an oblique-dominant environment eliminated perceptual biases across orientation. The results of these two additional adaptation conditions are shown in Figure 5 where the horizontal effect score has been plotted for the oblique-dominant and enhanced-natural conditions as well as the data from the same three observers in the isotropic adaptation condition reported in Figure 4. These additional data show a significantly different pre/post pattern of horizontal bias ($F(2,4) = 22.1$, $p = .007$ $\eta^2 = .917$): in the enhanced natural condition observers showed an increased anisotropy and in the oblique- dominant condition orientation perception was equalized (although the anisotropy was not reversed). That the diminution of the post-adaptation effect is

due to the post-adaptation test stimuli causing re-adaptation as opposed to simply due to the passage of time was shown in a control condition (Figure 6); after 30 minutes in the dark prior to beginning the post test, the adaptation effect was still observed at its full strength.

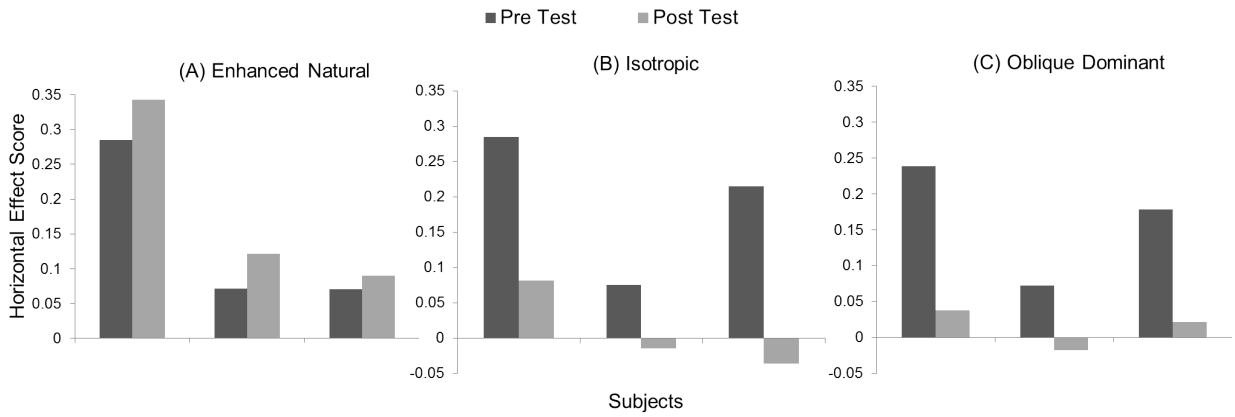

Figure 5. Measures of the horizontal effect for the three subjects who participated in all adaptation conditions (N=3).

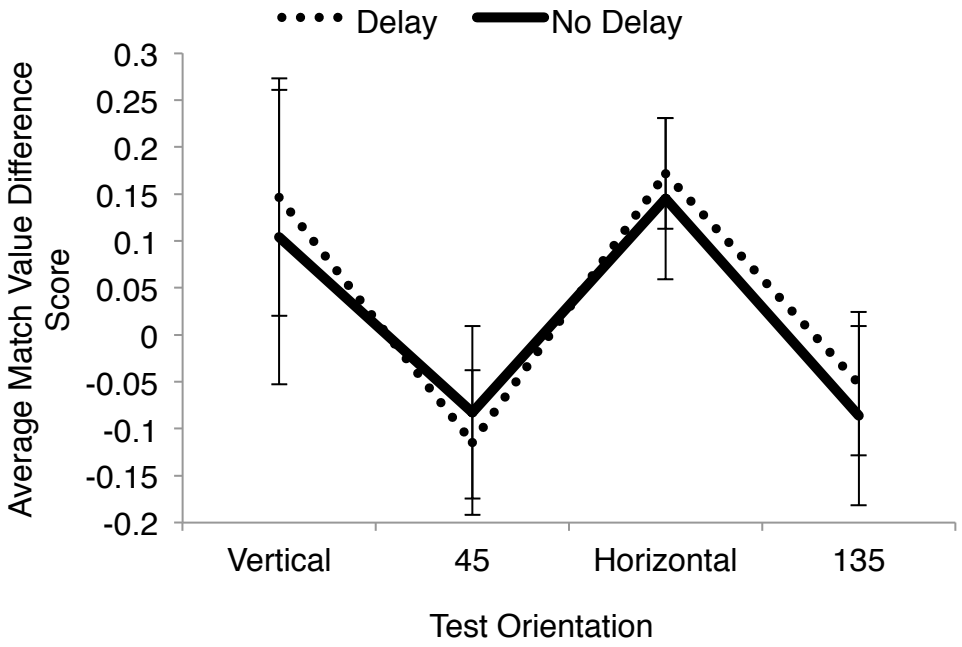

Figure 6. Observers' (N = 3) perceptual change after experience in an environment in which vertical content had been decremented by 85%. The post-test occurred either immediately following adaptation (solid line) or after a 30-minute delay in darkness (dotted line). The difference scores of subjects' pre-post match values are plotted. Error bars represented ±1 standard error.

Modeling

We used a Bayesian framework to model the change in observers' perception before and after adaptation. According to Bayes' theorem, the product of the likelihood distribution, $P(m|\boldsymbol{\theta})$, and the prior probability distribution, $P(\boldsymbol{\theta})$, is proportional to the posterior probability distribution, $P(\boldsymbol{\theta}|m)$, where $\boldsymbol{\theta}$ is the perceived orientation and m is the measured orientation of the stimulus. In an ideal encoder-decoder model, the observer makes a perceptual decision based on the posterior probability. The likelihood distribution is related to the measurement noise of the stimulus, can be derived from the precision of discrimination (Girshick, Landy, & Simoncelli, 2011; Stocker & Simoncelli, 2006), and has been shown to adapt in response to changes in the environmental input (Brenner, Bialek, & de Ruyter van Steveninck, 2000; Clifford et al., 2007; Dragoi, Sharma, & Sur, 2000). An ideal prior should be based on the environmental orientation distribution and can be related to perceptual bias (Girshick, Landy, & Simoncelli, 2011), one such perceptual bias being the behavioral horizontal effect (Essock et al. 2003; Hansen & Essock, 2004). Previous research has shown that recovered observers' priors are indeed biased across orientation and tend to match the environmental distribution, that is, peak at the two cardinal orientations (horizontal and vertical, Girshick, Landy, & Simoncelli, 2011). Adopting these methods, we modeled the differences in the likelihood and prior across experience in altered environments using the experimentally obtained perceptual variability to inform the likelihood (σ_{SCTest}) and modeled the bias (I_{SCTEst} - $I_{SCStandard}$) using a prior based on the environmental distribution.

Likelihood

We assume that observers use the correct likelihood function: the measurement noise distribution as a function of the stimulus for a particular perceptual judgment (Girshick, Landy, & Simoncelli, 2011). The standard deviation in the perceptual match value, as measured experimentally, is thus used to estimate the width of the likelihood function across orientation (Stocker & Simoncelli, 2006). Since our test is limited to discrete points on the orientation spectrum, we used cubic spline interpolation to estimate measurement noise across all orientations by fitting the experimentally obtained variability (standard deviation of match values: $[\sigma_0, \sigma_{45}, \sigma_{90}, \sigma_{135}, \sigma_{180}]$) at each test orientation before and after adaptation (Figure S1).

$$\sigma_{fitted} = a_i(\sigma - \sigma_i)^3 + b_i(\sigma - \sigma_i)^2 + c_i(\sigma - \sigma_i) + d_i$$

These interpolated data were then used to compute the width of the measurement distributions across orientation using a Von Mises distribution that peaks every 180 degrees:

$$P(m|\theta) \propto \frac{e^{K\cos(2(\theta-M))}}{2\pi I_o K}$$

where I_O is a modified Bessel function, K is determined by the fitted variability, σ_{fitted}, M ranges across orientation from 0-180°, and θ determines the peak of the Von Mises and is centered at the measured orientation. The likelihood as a function of orientation is extracted from this model of measurement space as shown in Figure S2 (pre-adaptation left, post-adaptation right). Vertical slices (columns) through the distribution space are the measurement distributions and horizontal slices (rows) are the likelihood distributions as a function of orientation (Girshick, Landy, & Simoncelli, 2011). As measurement distribution width varies across orientation, the likelihood functions are asymmetric. Moreover, the likelihood distribution post-adaptation is less peaked at horizontal (90^o) and more equal across orientation. This corresponds to the decreased sensitivity to horizontal and increased sensitivity to the obliques seen after adaptation in the experimental data (Figure 4).

Prior

To obtain an estimate of the prior before adaptation, we used the orientation spectra of over 350 natural images (Girshick, Landy, & Simoncelli, 2011). The spectra were calculated using the methodology detailed in our previous report (Schweinhart & Essock, 2013). Briefly, each image is rotated every three degrees and a discrete fast Fourier transform is performed. The amplitude spectrum (with the highest ~30% of frequencies discarded) is then convolved with a filter like those used to create the incremented noise images in the psychophysical task, centered at horizontal and vertical with a three-degree orientation bandwidth to extract the amplitude of those specific orientations at all spatial frequencies. As this process is repeated every three degrees for each image, the entire spectrum can be obtained by accumulating across the set of rotated images. To estimate the prior after adaptation, this method was also employed to calculate the average amplitude across orientation in the filtered videos recorded as people were adapting (see *Adaptation Paradigms and Analyses*, and Figure 3C). The prior should not be an exact match to the natural world, but rather a 'regularized' match in order to compensate for noisy environments (Feldman, 2013). Therefore, the fit of the prior both before and after

adaptation was estimated using cubic spline interpolation at 5 control points, θ = {0°, 45°, 90°, 135°, 180°}, and relaxed so as not to 'over-tune' (see Figure S3 for fits to data).

$$\log\left(P(\theta)\right) = \left(a_i(\theta-\theta_i)^3 + b_i(\theta-\theta_i)^2 + c_i(\theta-\theta_i) + d_i\right)^t$$

The relaxation process was accomplished by changing the temperature of the distribution, *t,* for each subject so as to best fit his/her specific perceptual results. The degree of relaxation was determined by a grid search over the values t = [.001,6] in increments of .001. The temperature parameter was independently set for each subject's prior and chosen so as to minimize squared error between the fit and the perceptual results (average exponents for natural: 2.07 and isotropic: .003)[3].

Bias

The experimental task measured observer bias: the physical difference between the salience of two orientations that were perceived to be equal. That is, subtracting the test orientation increment each subject needed to match that of the standard gives us a measure of relative bias across orientation ($I_{SCStandard} - I_{SCTest}$). Bias is approximately equal to the product of the squared likelihood width and the slope of the log of the prior (Girshick, Landy, & Simoncelli, 2011; Stocker & Simoncelli, 2006). The bias was estimated for each observer using the width (in degrees) of the modeled likelihood distributions at half height (FWHM) and the slope of the log of the prior (before and after adaptation) at five points (0°, 45°, 90°, 135°, 180°).

$$Bias_{model} = \left(\frac{\log\left(P(\theta)\right)-\log\left(P(\theta_i)\right)}{\theta-\theta_i}\right) FWHM(P(m|\theta))$$

The predicted bias values for these control points were then used to interpolate, again using cubic spline, across the range of orientations and compared to the bias obtained experimentally both before and after adaptation (Figures 7 and 8).

[3] Changing the temperature in this way effectively allowed the degree of anisotropic influence to be tailored to each subject. Note that raising the isotropic distribution to a decimal makes it even flatter while increasing the exponent of the natural distribution increases the anisotropy. Thus, the relaxation procedure did not change the pattern of anisotropy/isotropy, nor the relationship between orientations across the spectrum, but only the influence that the pattern of orientation in the environmental distribution had on each subject.

Modeling Results

It has been suggested that the prior represents the probability of encountering particular stimuli over a lifetime of past experience in the external world (Hansen, et al., 2015; Stocker & Simoncelli, 2006). However, previous results implicating a fixed prior have only investigated isolated changes to the distribution in the environment. We predicted that the change in observers' perception following isotropic adaptation might be better explained by a model that used the environmental distribution of orientations experienced during adaptation as the prior. Explicitly, we predicted that people would shift their prior to more accurately represent the orientation distribution in the recently experienced environment. We first modeled the pre-adaptation bias using the natural environmental distribution as prior and, as can be seen in Figure 7A, the model (lines with error plotted as the shaded region) provided a good fit to the data (points with error plotted as bars). To evaluate whether people were changing their prior probability distributions the model of post-adaptation perceptual bias was applied using both the natural orientation distribution (Figure 7B) and the isotropic orientation distribution (Figure 7C) as priors. As can be seen by comparing Figures 7B and C, the isotopic prior provided a better fit to human perceptual biases after isotropic experience as a function of orientation ($F(4,32) = 24.44$, $p < .001$ $\eta^2 = 0.33$).

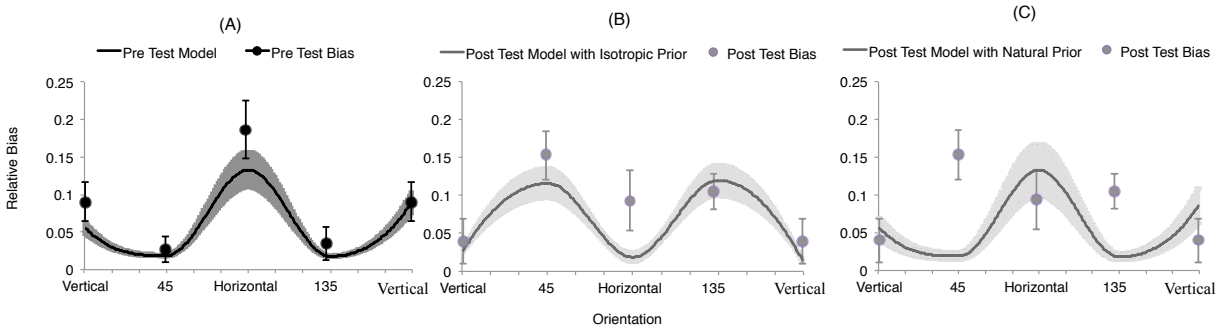

Figure 7. Experimentally-obtained bias and model fits of bias using a prior based on the natural orientation distribution across test orientation for pre (A) and post (B and C) test orientation bias and a likelihood derived from the experimental variability (N=9). Error bars and shaded areas represent standard error for empirically observed and simulated results, respectively.

The same procedures, including altering the prior distribution, were run for the enhanced natural and oblique-dominant environments and the fits of these models to the experimentally obtained data are shown in Figure 8. The modeled data fit the experimental findings well: the model fits the increased anisotropy in the enhanced-natural condition as well as the flatter

orientation perception in the oblique-dominant condition. The failure of the isotropic model to fully estimate the change at horizontal may suggest that horizontal is more resistant to change, but further testing would be needed to clarify this result. What is clear is that using the isotropic environment as the prior fits the experimentally obtained data much better than maintaining the natural anisotropic prior. Thus, perceptual biases after experience in a globally atypical environment are better explained by a prior that changes to reflect the *recently-experienced* environmental statistics.

Discussion

Some have suggested that the relationships between natural scene statistics and visual processing are most likely hardwired, perhaps reflecting the average of visual scenes experienced over millennia of evolution, in order to make the visual system an efficient information-transmitting system (Bex, Solomon, & Dakin, 2009; Brenner, Bialek, & de Ruyter van Steveninck, 2000; Stocker & Simoncelli, 2006; Webster & Miyahara, 1997). However, given the dynamic nature of processing the streaming visual world, a more useful strategy would be to optimize the encoding of incoming statistical information dynamically (Gutinsky & Dragoi, 2008; Wainwright, 1999). The present work indicates that observers have a representation of the regularities present in their recent environment and adjust their perception of features in the current scene context. While the distribution of orientations typically experienced leads to the horizontal-effect anisotropy of perceptual salience, we show that altering the recently experienced orientation distribution causes predictable changes in the perceptual salience of image structure. Indeed, experiencing scenes with a globally isotropic orientation spectrum causes observers' perception of orientation to become isotropic. Thus, perceptual encoding can adjust to the regularities in incoming signals such that the perceptual outcome is optimized to the most-current input.

One issue left to be addressed in future work is the relation of the duration of the adaptation to the magnitude of the effect observed. Also, in this study we filtered the image as a whole but more likely, these adaptation effects are regional, Thus, yet to be determined is, for a

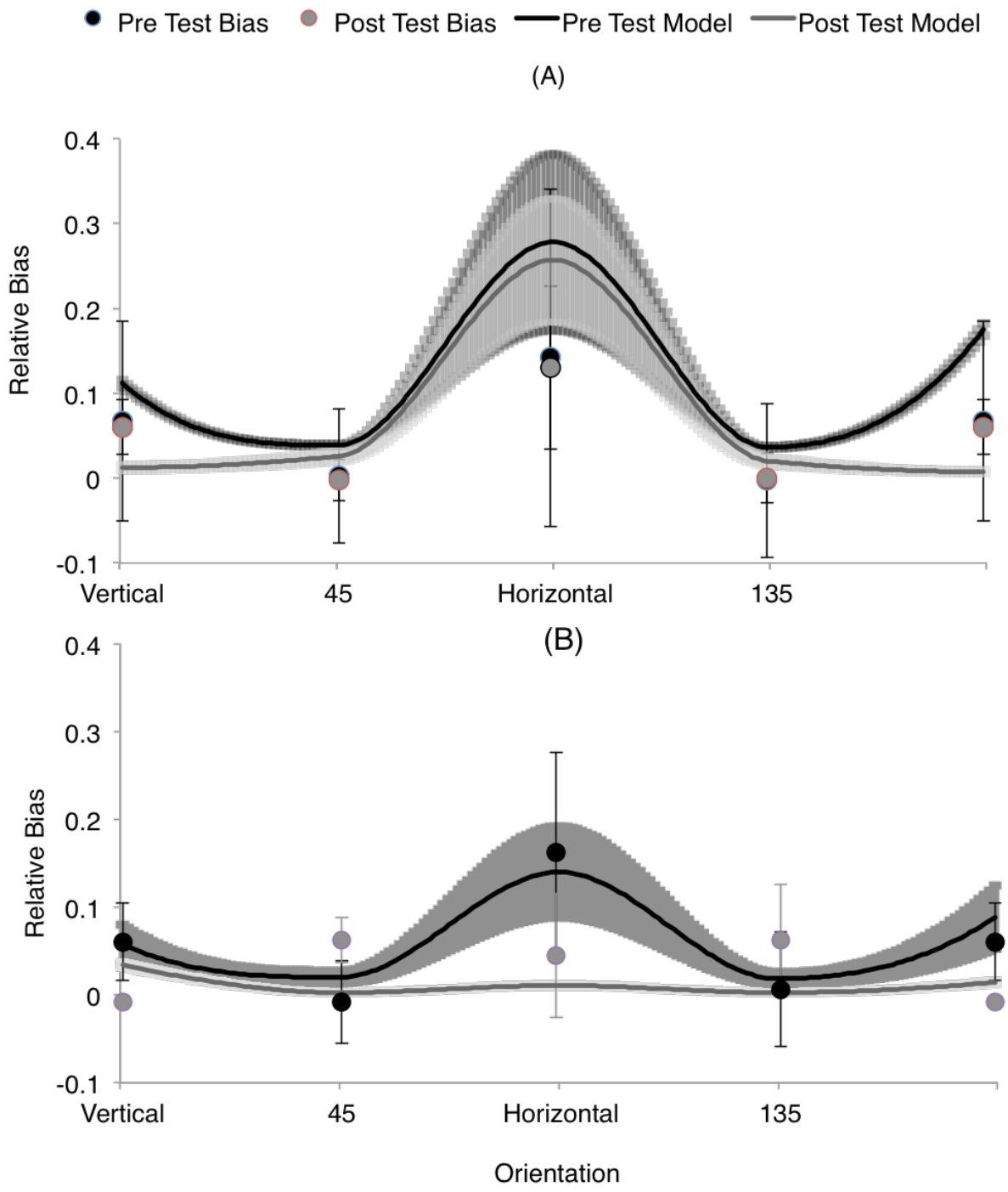

Figure 8. Experimentally obtained data and model for pre and post adaptation to the Enhanced-Natural (A) and Oblique-Dominant (B) conditions. Error bars and shaded regions show standard error (N=3).

particular test location, the spatial size of the region within which this adaptation occurs, as well as its spatiotemporal biases, and its variation with eccentricity. In addition, the role of random, coherent, or natural phase structure on the size of these effects is presently unknown (see e.g., Bex, 2010; Bex & Makous, 2002; Bex, Solomon, & Dakin, 2009).

Importantly, the changes we have shown appear to go beyond short-term changes in likelihoods (Stocker & Simoncelli, 2006), and implicate changes in the prior distributions. Our model is adapted from that used by Simoncelli and colleagues who have documented adaptation effects that are explained by changes in the likelihood alone (Girshick, Landy, & Simoncelli, 2011; Stocker & Simoncelli, 2006). The tilt aftereffect -- a decrease in variability and increase in bias observed after adaptation to an oriented stimulus -- is well explained by only changing the width of the likelihood in the vicinity of the adaptor value (Stocker & Simoncelli, 2006). Indeed, short adaptations would seem unlikely to elicit changes in prior beliefs which presumably reflect phylo- and ontogenetic experience with stable characteristics in the visual environment. Globally-altered environmental distributions, like those used here, provide a strong test of the malleability of priors. The local likelihood changes invoked to explain repulsive effects such as tilt aftereffect, are balanced by changes in the area around the adapted stimulus (Stocker & Simoncelli, 2006). For localized stimuli, this results in an increase in signal at the adapted stimulus and a slight decrease in surrounding regions. Adaption to globally-altered distributions, however, would require widespread changes to counteract areas where the prior deviates from the environmental distribution, In these cases, acknowledging the changed environmental distribution may lead to a simpler model. Indeed, as shown in Figure S2, the likelihood distributions do change in response to a globally-altered environmental distribution, becoming more homogeneous in terms of their variance. Alone, however, these likelihood changes cannot explain the behavioral changes observed in the experiment. The relatively isotropic pattern of perception requires that the prior also be change in a way that reflects the changes in the environment (Figure 7). Rather than being tuned to distributional information that presumably has been typical in visual environments for millennia, perceptual biases largely reflect an internal model in which both likelihood and priors adapt dynamically to recent experience.

Conclusion

Here we utilized virtual reality viewing to adapt observers to environments whose orientation spectrum had been artificially manipulated and showed that the experienced distribution of oriented content strongly altered which orientations of structure the observers saw best. Thus, rather than having been hardwired over millennia of experience of viewing presumably anisotropic scenes, the well-established bias in human perception of different orientations of image structure results from dynamic, on-the-fly, adjustment of perception. We suggest that suppression is differential across orientation to invert (and thereby whiten) the anticipated input based on recently-viewed scenes. These perceptual changes are predicted under a Bayesian framework wherein an observer's prior probability distribution across orientation changes to match the distributions of orientation in the recently-viewed scenes, thus serving to optimize orientation encoding based on the particular visual input just encountered.

Acknowledgments: We thank Stephen Engle and colleagues for advice and the use of their image acquisition and processing code and acknowledge the University of Louisville IRIG and GSRCA grants as well as the NSF CHS-1524888 for support.

References

Attick, J. J., & Redlich, A. N. (1990). Towards a theory of early visual processing. *Neural Computation*, *2*(3), 308-320.

Baddeley, R. J., & Hancock, P. J. (1991). A statistical analysis of natural images matches psychophysically derived orientation tuning curves. *Proceedings of the Royal Society of London B: Biological Sciences*, *246*(1317), 219-223.

Balikou, P., Gourtzelidis, P., Mantas, A., Moutoussis, K., Evdokimidis, I., & Smyrnis, N. (2015). Independent sources of anisotropy in visual orientation representation: a visual and a cognitive oblique effect. *Experimental brain research*, *233*(11), 3097-3108.

Bao, M., Fast, E., Mesik, J., & Engel, S. (2013). Distinct mechanisms control contrast adaptation over different timescales. *Journal of Vision*, *13*(10), 14.

Baud-Bovy, G., & Gentaz, E. (2012). The perception and representation of orientations: A study in the haptic modality. *Acta psychologica*, *141*(1), 24-30.

Barlow, H. (1989). Unsupervised learning. *Neural Computation, 1*(3), 295-311.

Bex, P. J. (2010). (In) Sensitivity to spatial distortion in natural scenes. *Journal of Vision, 10*(2):23, 1–15.

Bex, P. J., & Makous, W. (2002). Spatial frequency, phase, and the contrast of natural images. *JOSA A*, *19*(6), 1096-1106.

Bex, P.J., Solomon, S.G. & -Dakin, S.C. (2009). Contrast sensitivity in natural scenes depends on edge as well as spatial frequency structure. *Journal of Vision, 9*(10).

Brenner, N., Bialek, W., & de Ruyter van Steveninck, R. (2000). Adaptive rescaling maximizes information transmission. *Neuron, 26,* 695–702.

Cecchi, G.A., Rao, A.R., Xiao, Y., & Kaplan, E. (2010). Statistics of natural scenes and cortical color processing, *Journal of Vision, 10*(11), 21.

Clifford, C. W., Webster, M. A., Stanley, G. B., Stocker, A. A., Kohn, A., Sharpee, T. O., & Schwartz, O. (2007). Visual adaptation: neural, psychological and computational aspects. *Vision Research*, 47(25), 3125-3131

Coppola, D. M., Purves, H. R., McCoy, A. N., & Purves, D. (1998). The distribution of oriented contours in the real world. *Proceedings of the National Academy of Science*, *95*(7), 4002-4006.

Dragoi, V., Sharma, J., & Sur, M. (2000). Adaptation-induced plasticity of orientation tuning in adult visual cortex. *Neuron*, *28*(1), 287-298.

Essock, E. A. (1980). The oblique effect of stimulus identification considered with respect to two classes of oblique effects. *Perception*, *9*(1), 37-46.

Essock, E. A., DeFord, J. K., Hansen, B. C., & Sinai, M. J. (2003). Oblique stimuli are seen best (not worst!) in naturalistic broadband stimuli: A horizontal effect. *Vision Research, 43*(12), 1329-1335.

Essock, E. A., Krebs, W. K., & Prather, J. R. (1997). Superior sensitivity for tactile stimuli oriented proximally-distally on the finger: Implications for mixed class 1 and class 2 anisotropies. *Journal of Experimental Psychology: Human Perception and Performance*, *23*(2), 515.

Essock, E.A., Hansen, B.C., & Haun, A.M. (2007). Perceptual bands in orientation and spatial frequency: A cortical analogue to Mach bands. *Perception*, 36(5), 639-649.

Essock, E. A., Haun, A. M., & Kim, Y. (2009). An anisotropy of orientation-tuned suppression that matches the anisotropy of typical natural scenes. *Journal of Vision, 9*(1), 1-15.

Feldman, J. (2013). Tuning your priors to the world. *Topics in Cognitive Science*, 5(1), 13-34.

Field, D. J., & Brady, N. (1997). Visual sensitivity, blur and the sources of variability in the amplitude spectra of natural scenes. *Vision Research*, *37*(23), 3367-3383.

Girshick, A. R., Landy, M. S., & Simoncelli, E. P. (2011). Cardinal rules: visual orientation perception reflects knowledge of environmental statistics. *Nature Neuro., 14*(7), 926-156.

Gutnisky, D. A., & Dragoi, V. (2008). Adaptive coding of visual information in neural populations. *Nature*, 452(7184), 220-224.

Hansen, B. C., & Essock, E. A. (2004). A horizontal bias in human visual processing of orientation and its correspondence to the structural components of natural scenes. *Journal of Vision, 4*(12), 1044-1060.

Hansen, B., & Essock, E. (2005). Influence of scale and orientation on the visual perception of natural scenes. *Visual Cognition*, *12*(6), 1199-1234.

Hansen, B. C., & Essock, E. A. (2006). Anisotropic local contrast normalization: The role of stimulus orientation and spatial frequency bandwidths in the oblique and horizontal effect perceptual anisotropies.*Vision research*, *46*(26), 4398-4415.

Hansen, B. C., Richard, B., Andres, K., Johnson, A. P., Thompson, B., & Essock, E. A. (2015). A cortical locus for anisotropic overlay suppression of stimuli presented at fixation. *Visual Neuroscience*, 32.

Hancock, P. J., Baddeley, R. J., & Smith, L. S. (1992). The principal components of natural images. *Network: Computation in neural systems*, *3*(1), 61-70.

Keil, M. S., & Cristóbal, G. (2000). Separating the chaff from the wheat: Possible origins of the oblique effect. *Journal of the Optical Scoiety of America A*, *17*(4), 697-710.

Maloney, R. T., & Clifford, C. W. (2015). Orientation anisotropies in human primary visual cortex depend on contrast. *NeuroImage*, *119*, 129-145.

Morgan, M. J., Ross, J., & Hayes, A. (1991). The relative importance of local phase and local amplitude in patchwise image reconstruction. *Biological Cybernetics*, *65*(2), 113-119.

Schweinhart, A. M., & Essock, E. A. (2013). Structural content in paintings: Artists overregularize oriented content of paintings relative to the typical natural scene bias. *Perception*, *42*, 1311-1332.

Shapley, R., Caelli, T., Grossberg, S., Morgan, M., & Rentschler, I. (1990). Computational theories of visual perception. In Spillmann L. Werner J. S. (Eds.), *Visual perception. The neurophysiological foundations* (pp. 417–448). San Diego, CA: Academic Press.

Shepard, R. N. (1992). The perceptual organization of colors: an adaptation to regularities of the terrestrial world? In Barkow, Jerome H; Cosmides, Leda; Tooby, John (Eds.), *The adapted mind: Evolutionary psychology and the generation of culture*, (pp. 495-532). New York, NY, US: Oxford University Press.

Smyrnis, N., Mantas, A., & Evdokimidis, I. (2014). Two independent sources of anisotropy in the visual representation of direction in 2-D space. *Experimental brain research*, *232*(7), 2317-2324.

Stocker, A., & Simoncelli, E. P. (2006). Sensory adaptation within a Bayesian framework for perception. *Advances in Neural Information Processing Systems,* eds Weiss, Y. Schoelkopf, B., Platt, J. (Cambridge, MA: MIT Press), pp. 1291–1298.

Switkes, E., Mayer, M. J., & Sloan, J. A. (1978). Spatial frequency analysis of the visual environment: Anisotropy and the carpentered environment hypothesis. *Visison Research*, *18*(10), 1393-1399.

Wainwright, M. J. (1999). Visual adaptation as optimal information transmission. *Vision Reearch., 39*(23), 3960-3974.

Webster, M. A., & Miyahara, E. (1997). Contrast adaptation and the spatial structure of natural images. *Journal of the Optical Society of America*, *14*(9), 2355-2366.

Webster, M. A., & MacLeod, D. I. (2011). Visual adaptation and face perception. *Philosophical Transactions of the Royal Society B: Biological Sciences*, **366**(1571), 1702-1725.

Webster, M. A., Werner, J. S., & Field, D. J. (2005). Adaptation and the Phenomen of Perception. In *Fitting the mind to the world: Adaptation and aftereffects in high level vision.* (Oxford: Oxford University Press, 2005). Vol. 2.

Zhang, P., Bao, M., Kwon, M., He, S., & Engel, S.A. (2009). Effects of orientation-specific visual deprivation induced with altered reality. *Current Biology, 19,* 1956-1960.

Supplementary Figures

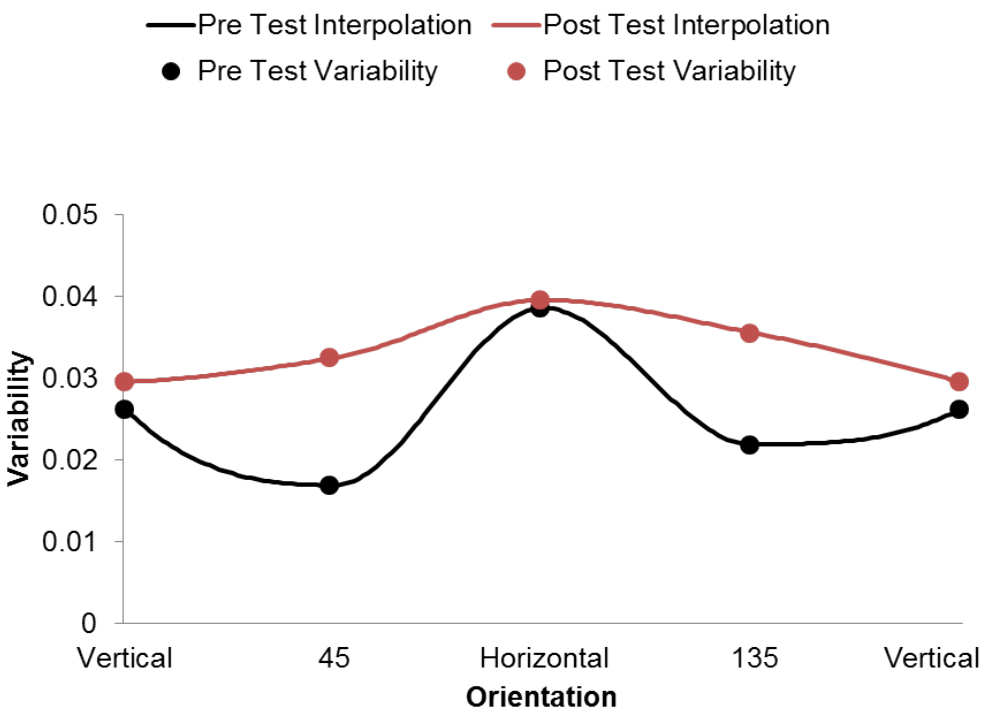

Figure S1. Variability in the pre- and post-test conditions used to model measurement distribution widths (N=9).

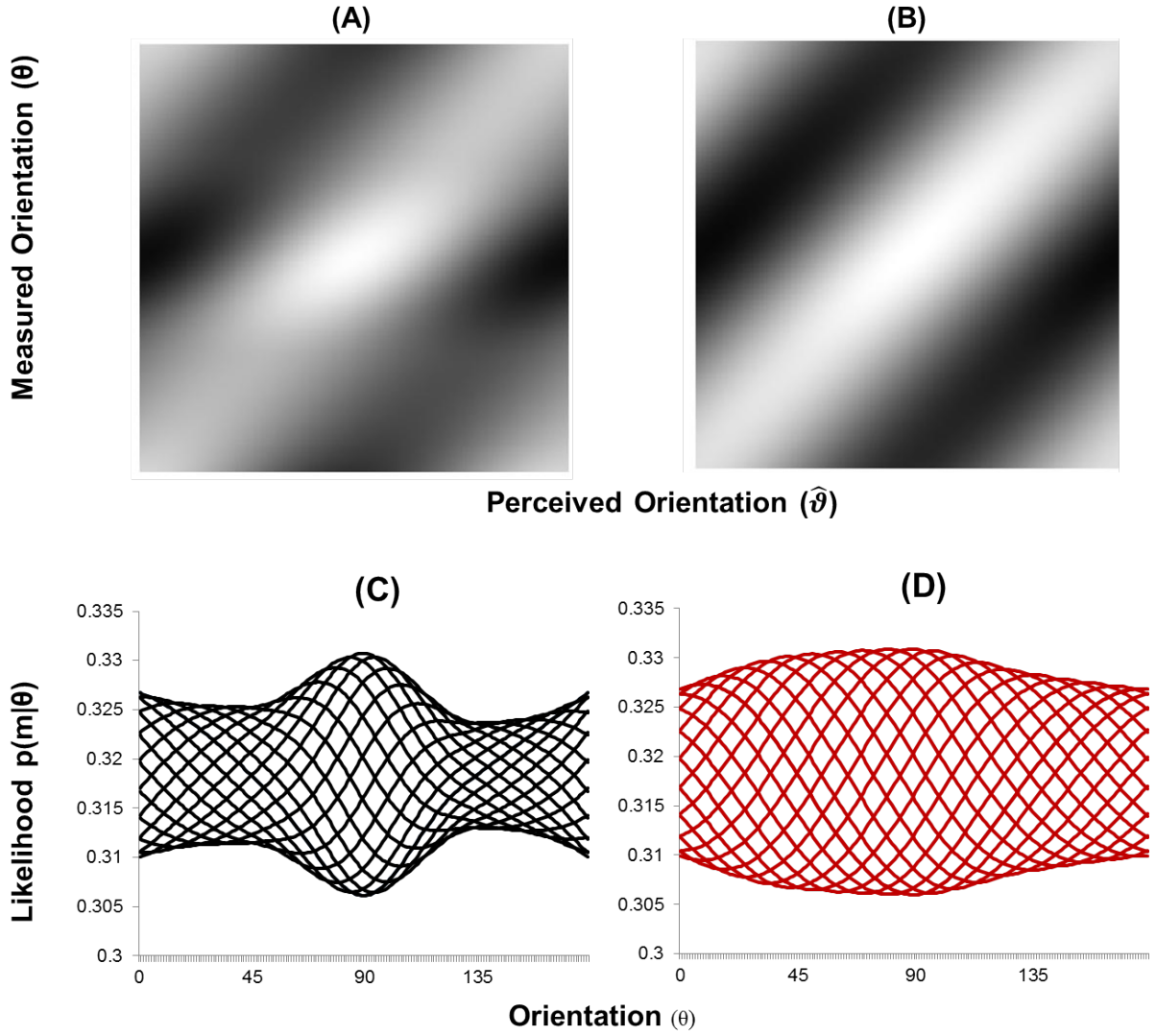

Figure S2. (A) and (B) show the measurement spaces modeled across orientation for the baseline and post-adaptation condition, respectively. (C) and (D) show the corresponding horizontal slices (every 10°) through these measurement spaces: the likelihood distributions pre (C) and post (D).

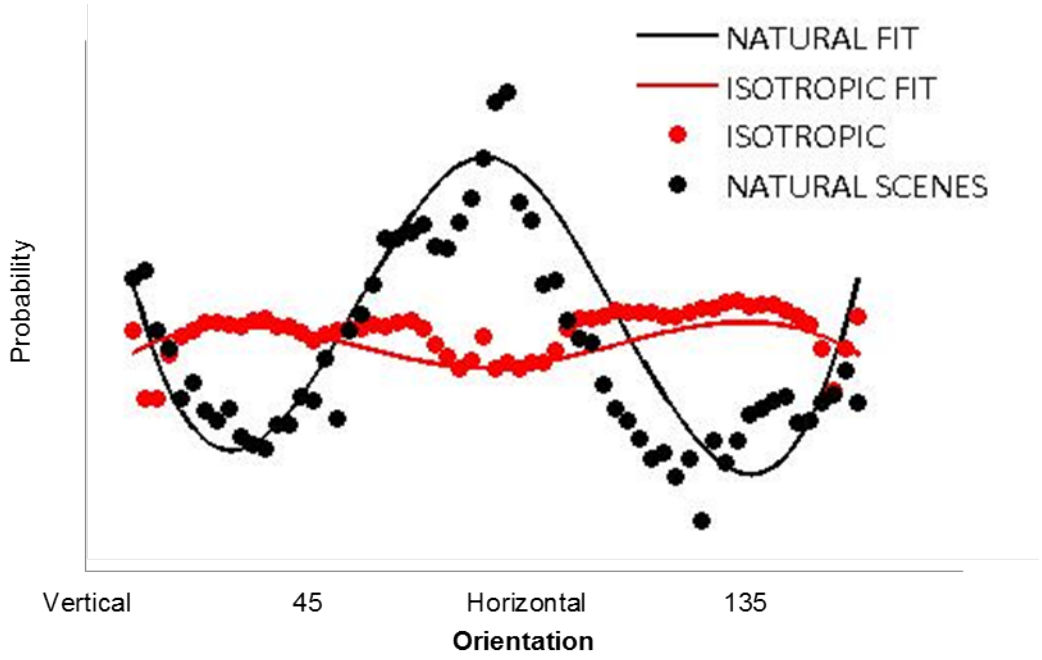

Figure S3. Discrete data points and interpolation used to model the natural (black) and isotropic (red) priors, respectively.